

# Simulation Research on Aerodynamic of Railway Freight Train Based on CFD Method

Yujiang XIE <sup>a,1</sup> and Zhenfeng WU <sup>a</sup>

<sup>a</sup>*Mechanical and Electrical Engineering of Lanzhou Jiaotong University, Lanzhou, Gansu, China*

**Abstract.** Some areas of the Lanzhou-Xinjiang Railway are accompanied by strong crosswinds all the year. The lateral force it generates pose a threat to the safe operation of railway freight trains. This paper conducts a numerical simulation study on three freight trains under five crosswind angles by using CFD method in order to aiming at the relationship between the crosswind angle and the aerodynamic force. The SIMPLE algorithm is used to solve the Reynolds-averaged N-S equation and the SST  $k-\omega$  model is used for the turbulence model. The research results include the variation of the aerodynamic force on the three freight trains with the crosswind angle and the variation of the aerodynamic force on each train. In addition, this paper discusses the pressure and flow field distribution around the freight train. The results of this paper provide a reference for the safe operation of Lan-Xin Railway.

**Keywords.** Railway freight train, CFD method, crosswind angle, aerodynamic performance, numerical simulation

## 1. Introduction

Lan-Xin Railway is an important passage for freight transportation in China. Due to its special geographical location, Lan-Xin Railway has passed through many wind areas, which have harsh environment and strong crosswinds all year round. It poses a threat to the safe operation of freight trains [1]. Although some scholars have studied the relationship between crosswind angle and aerodynamic performance of the train, these studies usually focus on the field of high-speed trains. In addition, these studies are mainly for the whole vehicle, but do not consider the changes in the aerodynamic force of each vehicle [2-3]. Freight trains and high speed trains are very different in cross sectional shape or running speed, so it is necessary to consider the influence of crosswind angle on the aerodynamic of each freight train. Aiming at the common freight trains on Lan-Xin Railway, this paper studies the influence of crosswind angle on the aerodynamic performance of each gondola car, boxcar and tank car.

---

<sup>1</sup> Yujiang Xie, Corresponding author, Mechanical and Electrical Engineering of Lanzhou Jiaotong University, Lanzhou, Gansu, China; E-mail: 2067382109@qq.com.

## 2. Research Methods

### 2.1. Fluid Basic Governing Equations

Continuity equation, momentum conservation equation and energy conservation equation are the basic equations governing fluid flow [4]. In this paper, the air is incompressible, the heat exchange between the incompressible flows is very small, so the energy conservation equation is not considered in this paper. For constant flow, the continuity equation without considering fluid compressibility is:

$$\frac{\partial(\rho u_j)}{\partial x_j} = 0 \quad (1)$$

In the formula (1),  $\rho$  represents the fluid density;  $u_j (j=1,2,3)$  represents the component of the velocity vector  $\mathbf{u}$  in the direction  $x_j$  in the Cartesian coordinate system. The momentum conservation equation is:

$$\frac{\partial(\rho u_i)}{\partial t} + \frac{\partial(\rho u_i u_j)}{\partial x_j} = -\frac{\partial p}{\partial x_i} + \frac{\partial \tau_{ij}}{\partial x_j} \quad (2)$$

In the formula (2),  $p$  represents the pressure acting on the fluid micro-element;  $\tau_{ij}$  represents the viscous stress tensor acting on the micro-element due to molecular viscosity. Computational fluid dynamics (CFD) can accurately simulate turbulent flow [5]. In this paper, the software Fluent is used for numeral calculations, the turbulence model is the SST  $k-\omega$  model, the SIMPLE algorithm is used to solve the Reynolds-averaged N-S equation, and the second-order upwind formula is used to discretize it.

### 2.2. Geometric Model and Meshing

A certain type of electric locomotive is selected as the research object for pulling gondola cars, boxcars and tank cars. The geometric model is a locomotive towing three freight cars, ignoring the pantograph of the locomotive, and appropriately simplifying the bogie of the locomotive. Mesh quality is very important to the convergence of simulation calculation and the accuracy of results [6]. Due to the complex shape of the freight train, this paper uses workbench meshing to perform unstructured meshing, and locally densifies areas such as the car body surface and bogie. There are 12 boundary layers in total, the value is controlled at 30-100. The surface meshes of locomotives and wagons are shown in figures 1(a)-(d).

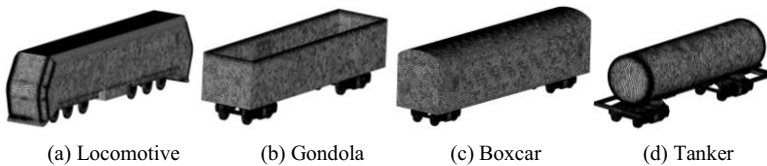


Figure 1. Surface meshes of locomotives and wagons.

2.3. Calculation Conditions

At present, there are two ways to simulate the operation of freight trains under the action of crosswind, one is the synthetic wind method, and the other is the dynamic grid method [7]. This paper uses the synthetic wind method. Since the wind direction of Lan-Xin Railway is relatively fixed, and most of the crosswind angles are 60°-120°, so the crosswind angles in this paper are set to 60°, 75°, 90°, 105° and 120°. The crosswind angle  $\beta$  is shown in figure 2.

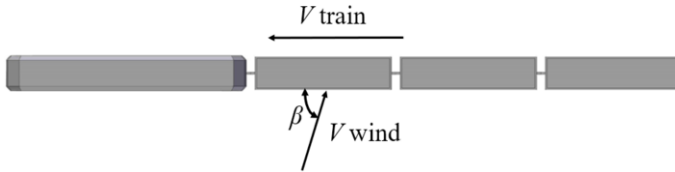


Figure 2. The crosswind angle  $\beta$ .

Some studies have shown that trains are prone to overturning when running on double-track embankments [8]. At present, there are few studies on the aerodynamic of freight trains under the condition of double line embankment. Therefore, in the environmental condition of this paper, freight trains are selected to run on the double line embankment, and the embankment height is set to 6m. The double line embankment is shown in figure 3.

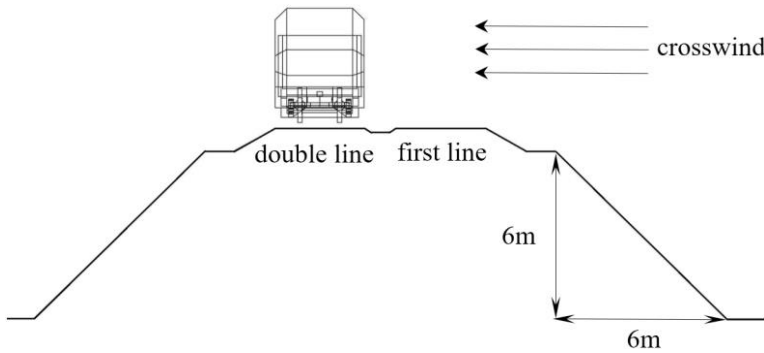


Figure 3. The double line embankment.

The calculation condition of this paper is to research the influence of the crosswind angle on the aerodynamic performance of each train under a certain train speed and crosswind speed. The data of velocity inlet  $V_x$  and  $V_y$  under different crosswind angles are shown in table 1.

Table 1. Velocity inlet data at different crosswind angles.

Crosswind angle	Train speed (km/h)	Crosswind speed (m/s)	$V_x$ (m/s)	$V_y$ (m/s)
60°	90	25	37.5	21.65
75°	90	25	31.47	24.15
90°	90	25	25	25
105°	90	25	18.53	24.15
120°	90	25	12.5	21.65

2.4. Computational Domain and Boundary Conditions

In this paper, the size and boundary conditions of the computational domain are set reasonably with reference to the numerical simulation specification for the aerodynamic performance of trains. The train computational domain is a cuboid; the ground and embankment are set as sliding walls equal to the train running speed with opposite directions; the top surface is set as a symmetric boundary; the car body surface is set as a non-slip wall; the outlet condition is the pressure outlet and the far-field pressure is standard atmospheric pressure. The size of the computational domain is shown in figure 4, where  $h$  represents the height of the locomotive (4.08m).

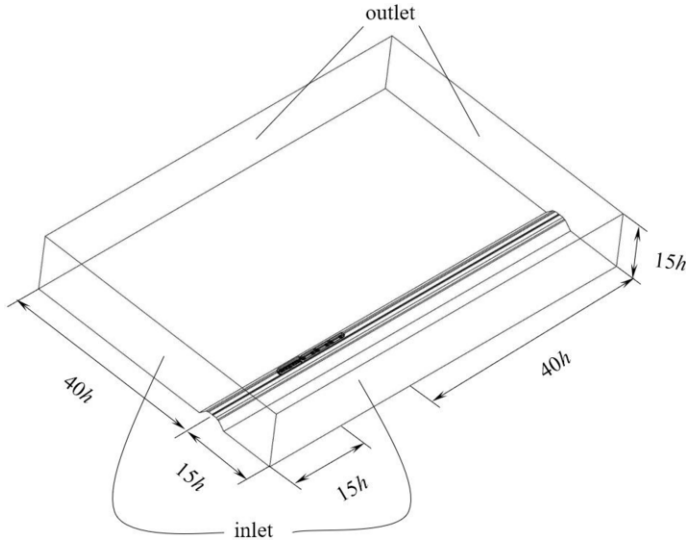


Figure 4. Model computation domain.

2.5. Method Feasibility Verification

In order to verify the correctness of the method adopted, this paper refers to the wind tunnel test data measured by the Central South University team for feasibility verification [9]. The comparison between the calculated data and the wind tunnel experiment data in the literature is shown in figure 5.

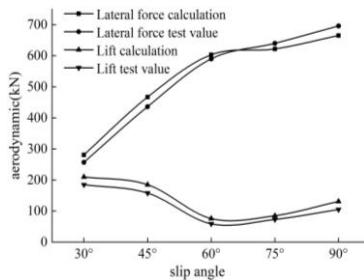


Figure 5. Comparison of calculated data and literature data.

Figure 5 shows that the calculated lateral force and lift are in good agreement with the experimental results in the literature. Therefore, the model and numerical calculation method selected in this paper are considered feasible.

2.6. Grid Independence Verification

In order to verify that the number of grids selected in this paper is reasonable, three groups of grids with different numbers are selected for calculation. The grid independent verification data is shown in table 2.

Table 2. Grid independent verification data.

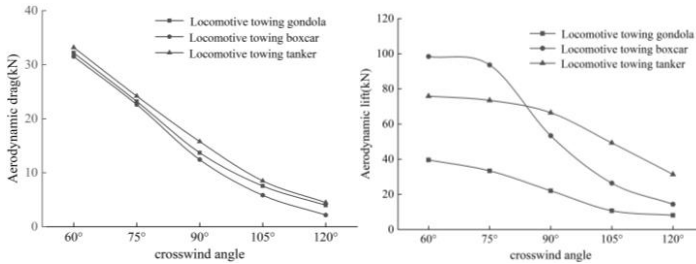
Number of grids(million)	Aerodynamic drag(kN)	Aerodynamic lift(kN)	Lateral force(kN)
28.15	15.774	66.454	132.251
30.77	15.912	65.297	132.576
33.63	15.613	67.134	132.118

Table 2 shows that with the increase of the grids number, the change of the train aerodynamic force is always within 2%, Therefore, grids around 28 million meet the computational requirements.

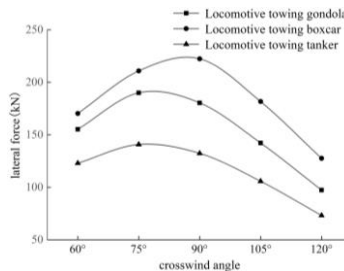
3. Calculation Results and Discussion

3.1. Aerodynamic Analysis

The aerodynamic force of the train towing the freight car at different crosswind angles are shown in figure 6.



(a) Aerodynamic drag at different crosswind angles (b) Aerodynamic lift at different crosswind angles



(c) Lateral force at different crosswind angles

Figure 6. Aerodynamic force at different crosswind angles.

Figure 6(a) shows that the drag of the three trains decreases with the increase of the crosswind angle, and the difference between them is close. The aerodynamic drag of the tank car is the largest, followed by the gondola car, and the boxcar is the smallest. Figure 6(b) shows that the lift of the three trains decreases with the increase of the crosswind angle, but the difference between them is large. Boxcars have the largest lift at  $60^{\circ}$ - $75^{\circ}$  crosswind angles; tank cars have the largest lift at  $90^{\circ}$ - $120^{\circ}$  crosswind angles; gondola cars always have the smallest lift. The lift of the tank car and the gondola car is relatively stable, and they both decrease steadily with the increase of the crosswind angle; the lift of the boxcar is relatively drastic, and they decrease rapidly under the crosswind angle of  $75^{\circ}$ - $105^{\circ}$ . Figure 6(c) shows that with the increase of the crosswind angle, the lateral forces on the three types of trains first increase and then decrease. Boxcars are subjected to the largest lateral force, followed by gondolas, and tank cars are the smallest. Notably, boxcars suffer the greatest lateral force at the  $90^{\circ}$  crosswind angle, while gondolas and tankers are at the  $75^{\circ}$ . The lateral forces suffered by three trains under the  $60^{\circ}$ - $90^{\circ}$  crosswind angle are significantly higher than  $90^{\circ}$ - $120^{\circ}$ .

The above conclusions are all for the whole vehicle, and do not involve changes in the aerodynamic force of each truck. Due to the low speed of freight trains, the influence of aerodynamic drag on the aerodynamic performance of the train is very limited. In addition, the weight of the freight train is relatively large, so the aerodynamic lift will not affect the safe operation of the freight train. What can threaten the safe operation of freight trains is the lateral force on each train. Therefore, this paper ignores the changes of aerodynamic drag and aerodynamic lift for each vehicle. Figure 7 shows the lateral force on each vehicle under different crosswind angles.

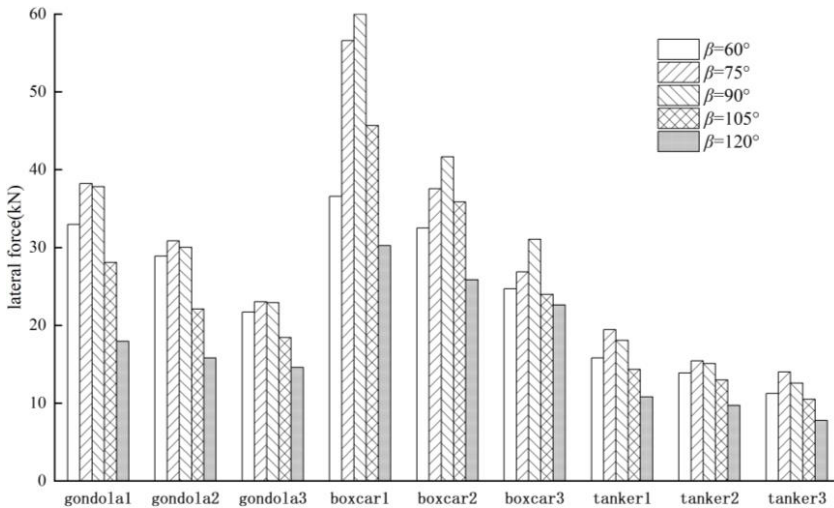
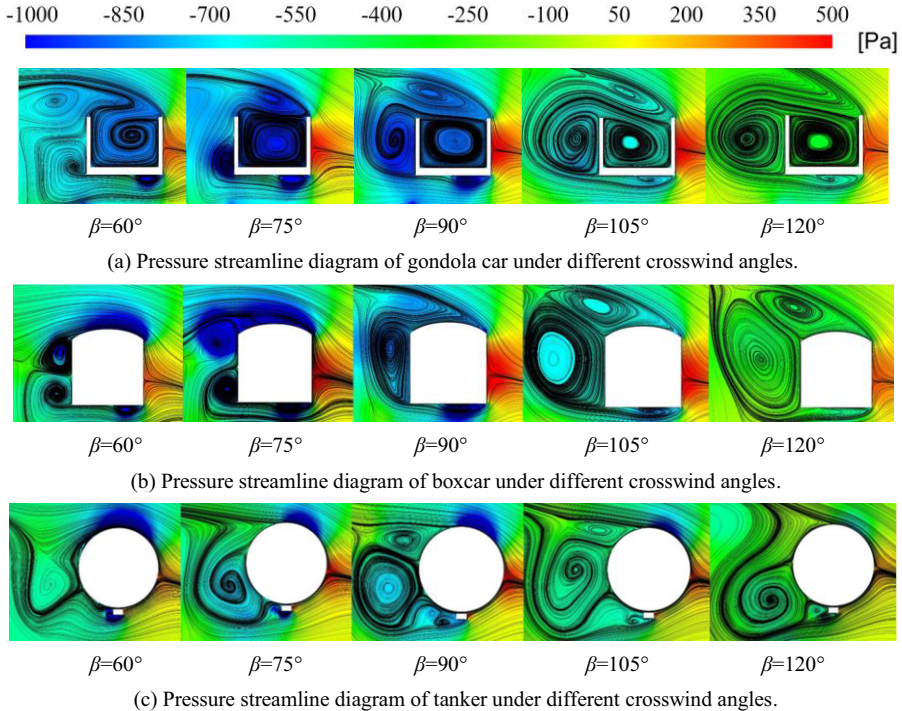


Figure 7. Lateral force of each vehicle under different crosswind angles.

Figure 7 shows that the lateral force on the first car is the largest, followed by the second car, and the third car is the smallest. With the increase of the crosswind angle, the lateral force of each vehicle first increases and then decreases. Under the same crosswind angle, the maximum difference in the lateral force of each gondola car is 39.4%, the box car is 52.5%, and the tank car is 30.4%.

### 3.2. Analysis of Pressure Flow Field

In order to study the effect of crosswind angle on the aerodynamic performance of freight trains, this paper studies the pressure and flow field distributions of three freight cars under five crosswind angles for the middle section of the first car. The pressure and flow field distributions of the gondola car, boxcar, and tank car under different crosswind angles are shown in figures 8(a)-(c).



**Figure 8.** Pressure streamline diagram of truck under different crosswind angles.

Figure 8 shows that there is negative pressure on the roof of all cars, which is a key factor affecting lift. The roofs of boxcars and tankers are arc-shaped. When the air flows through the roof, the flow rate increases and the pressure decreases, so the lift is larger. Due to the rectangular cavity at the top of the gondola, the flow velocity in the cavity is low and the pressure is high, so the lift experienced by the gondola is smaller than boxcar and tank car. With the increase of the crosswind angle, the negative pressure of the train roof gradually decreases, corresponding to figure 6(b), which is an important reason to explain the lift force gradually decreases with the increase of the crosswind angle. With the increase of the crosswind angle, the pressure difference between the windward side and the leeward side of the vehicle body first increases and then decreases, they reached the maximum value at the  $75^\circ$  and  $90^\circ$  crosswind angles, corresponding to figure 6(c). This is an important reason for the largest lateral force on the vehicle at  $75^\circ$  and  $90^\circ$  crosswind angles. For the gondola car, the surface of the gondola car is flat, the edges and corners are distinct, so the air flow is easy to gather and they can form a clear vortex. For the box car, although the roof of the box car is an

arc surface, the side of the car body is very flat, so the airflow can also form a clear vortex. For the tankers, the tankers are all arc surfaces except bogies, so it is difficult for the air to gather and it is difficult for the airflow to form a vortex under the  $60^\circ$  crosswind angle.

In order to study the change of the aerodynamic performance of each freight car under the same crosswind angle, this paper studies the pressure and flow field distribution of three freight trains based on the horizontal section of the freight train. The flow field distributions are shown in figures 9(a)-(c).

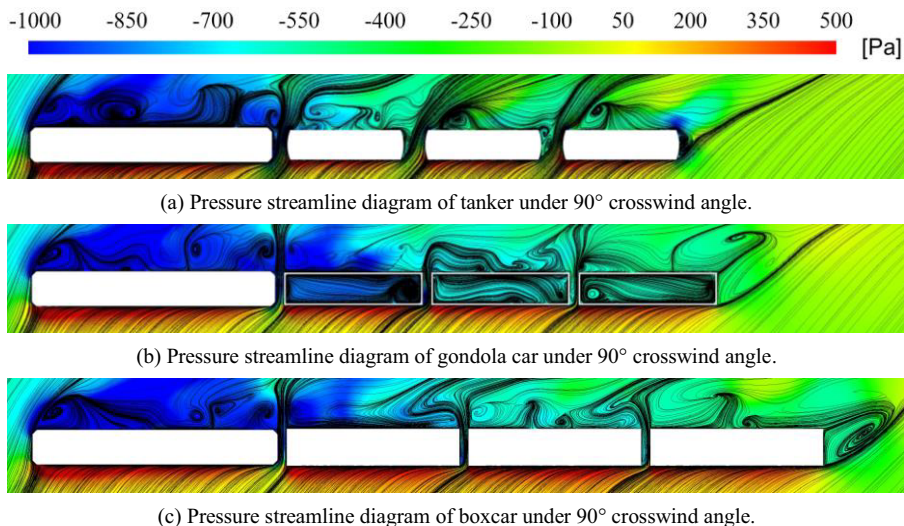


**Figure 9.** Streamline diagram of vehicle pressure under  $90^\circ$  crosswind angle.

Figure 9 shows that there is positive pressure on the windward side of all vehicles and negative pressure on the leeward side, which is an important reason for the lateral force. Among the three models, the pressure difference between the gondola and the boxcar is larger, and the pressure difference between the tank car is the smallest. The box car has the largest volume and the largest force area, so the box car has the largest lateral force; the tank car has a special shape, and the actual force area is the smallest, so the tank car has the smallest lateral force. At the same crosswind angle, the pressure difference between the windward side and the leeward side decreases gradually as the position moves backward. This also explains the reason why the first car in figure 7 has the largest lateral force and the third car is the smallest. It is worth noting that compared with the gondola car and the boxcar, the pressure on the side of each tank car is relatively similar, which explains the reason why the lateral force on each tank car in figure 7 is the closest.

Due to the difference between the shapes, gondolas and boxcars have larger wakes, and tank cars have smaller wakes. It is worth noting that the air creates one larger vortex on the lee side of the tanker, while it creates multiple smaller vortices on the lee side of the gondola and boxcar. The distance between each tank car is large and the air can flow through the gap smoothly, so it forms a large vortex on the leeward side of the tanker which consumes energy. The distance between each gondola car and boxcar is

small, some of the energy is lost as the air flows through the gap, so less vortex is formed on the leeward side.

#### 4. Conclusion

In this paper, the aerodynamic performance of three freight trains under five typical crosswind angles is investigated by CFD method. The research results include the variation of the aerodynamic force on the three freight trains with the crosswind angle and the variation of the aerodynamic force on each train. In addition, this paper discusses the pressure and flow field distribution around the freight train. The results of this paper provide a reference for the safe operation of Lan-Xin Railway.

#### Acknowledgements

The authors gratefully acknowledge the support for this research provided by Gansu Provincial Department of Science and Technology under Research Grant No. 20YF3GA014.

#### References

- [1] Jiang P, Pan XM, Xue JM and Sha YP. Comparative analysis of strong wind characteristics in the strongest wind area along the Xinjiang railway. *Journal of Meteorology and Environment*. 2020; 36(05): 69-75
- [2] Xi YH, Mao J, Li MG, Zhang N and Ma XY. Numerical simulation of crosswind effect of high-speed train. *Journal of Beijing Jiaotong University*. 2010; 34(01): 14-19
- [3] Mao J, Xi YH and Yang GW. Research on the effect of crosswind wind field characteristics on the aerodynamic performance of high-speed trains. *Railway Journal*. 2011; 33(04): 22-30
- [4] Tianyu L and Sichen T. *Fluid mechanics*. Chongqing: Chongqing University Press. 2018; p.15-18
- [5] Xiaosheng W and Xiaopeng H. *Fundamentals of computational fluids*. Beijing: Beijing Institute of Technology Press. 2021; p. 46
- [6] Li T, Qin D, An C and Zhang JY. Influence of computational grid on train aerodynamic uncertainty. *Journal of Southwest Jiaotong University*. 2019; 54(04) 816-822
- [7] Premoli A, Rocchi D, Schito P and Tomasini G 2016 Comparison between steady and moving railway vehicles subjected to crosswind by CFD analysis. *Journal of Wind Engineering & Industrial Aerodynamics*. 2016; 156(01): 29-40
- [8] Zhu HY, Wang YH, Zhu ZH, Yuan Y and Zen J. Influence of the height of the embankment on the aerodynamic performance of high-speed trains under cross winds. *Chinese Journal of Transportation Engineering*. 2021; 21(06): 181-193
- [9] Zhou D, Tian HQ, Yang MZ and Lu ZJ. Comparison of aerodynamic performance of different types of railway freight cars running on the embankment of Qinghai-Tibet railway under strong crosswind. *Journal of Railways*. 2007; 29(05): 32-36